RESEARCH ARTICLE

k-t BLAST and SENSE accelerated time-resolved three-dimensional phase contrast MRI in an intracranial aneurysm

Pim van Ooij · Annetje Guédon · Henk A. Marquering ·
Joppe J. Schneiders · Charles B. Majoie ·
Ed van Bavel · Aart J. Nederveen

Abstract

Objective The objective of this study was to investigate the performance of *k-t* BLAST (Broad-use Linear Acquisition Speed-up Technique) accelerated time-resolved 3D PC-MRI compared to SENSE (SENSitivity Encoding) acceleration in an in vitro and in vivo intracranial aneurysm.

Materials and methods Non-accelerated, SENSE and *k-t* BLAST accelerated time-resolved 3D PC-MRI measurements were performed in vivo and in vitro. We analysed the consequences of various temporal resolutions in vitro.

Results Both in vitro and in vivo measurements showed that the main effect of *k-t* BLAST was underestimation of velocity during systole. In the phantom, temporal blurring decreased with increasing temporal resolution. Quantification of the differences between the non-accelerated and accelerated measurements confirmed that in systole SENSE performed better than *k-t* BLAST in terms of mean velocity magnitude. In both in vitro and in vivo measurements, *k-t* BLAST had higher SNR compared to SENSE. Qualitative comparison between measurements showed good similarity.

Conclusion Comparison with SENSE revealed temporal blurring effects in *k-t* BLAST accelerated measurements.

Keywords *k-t* BLAST · Phase Contrast MRI · Intracranial aneurysm · Phantom

P. van Ooij (✉) · A. Guédon · H. A. Marquering ·
J. J. Schneiders · C. B. Majoie · A. J. Nederveen
Department of Radiology, Academic Medical Center,
University of Amsterdam, Meibergdreef 9, 1105 AZ Amsterdam,
The Netherlands
e-mail: pim.vanooij@gmail.com

P. van Ooij · A. Guédon · H. A. Marquering · E. van Bavel
Department of Biomedical Engineering and Physics,
Academic Medical Center, Amsterdam, The Netherlands

Abbreviations

PC-MRI	Phase contrast MRI
k-t BLAST	Broad-use linear acquisition speed-up technique
SENSE	Sensitivity encoding
FFE	Fast field echo
TOF	Time of flight
NSA	Number of signal averages

Introduction

Ruptured intracranial aneurysms constitute a major cause of subarachnoid haemorrhage, leading to a mortality rate up to 83 % [1] or high morbidity. To prevent rupture of incidentally found aneurysms, endovascular coiling or surgical clipping are considered. However, both interventions have substantial mortality and morbidity risks, and are expensive [2]. An accurate estimation of risk of rupture is therefore needed to come to an optimal treatment decision. It is believed that apart from size and morphology of the aneurysm, hemodynamic parameters such as inflow jet size, impingement zone and wall shear stress contribute significantly to rupture risk assessment [3].

Estimations of hemodynamics within aneurysms are mostly obtained using Computational Fluid Dynamics (CFD), an extensively validated simulation technique. However, this approach is hampered by long computational times and various assumptions such as the use of non-patient-specific boundary conditions [4].

Another, direct and non-invasive, technique for measurement of intracranial aneurysm hemodynamics is time-resolved three-dimensional phase contrast MRI (PC-MRI) [5]. It has been shown that PC-MRI can be used to assess hemodynamic properties in intracranial aneurysms [6–10].

However, for a number of reasons long scanning times are needed. A spatial resolution is needed that is sufficient to estimate local velocity patterns. Temporal resolution needs to be high enough to record peak systolic velocities. The signal-to-noise ratio (SNR) needs to be as high as possible to maximize blood-flow direction certainty and the accuracy of blood flow quantification [6]. Finally, at least three flow-sensitized acquisitions are needed to resolve x, y and z components of the flow velocity, as well as one flow compensated acquisition to remove unwanted background phases due to main field inhomogeneities, eddy currents and other factors [7]. In order to reduce scanning times for PC-MRI to clinically feasible durations with these conditions, acceleration techniques are required.

PC-MRI imaging time can be reduced by accelerated parallel imaging and reconstruction techniques, e.g., SENSE [8]. In SENSE, the scan times decrease in proportion to the acceleration factor. However, SNR decreases in proportion to the square root of the SENSE acceleration factor times the coil geometry factor g. It has been shown by Thunberg et al. [9] that at high acceleration factors the SNR of the magnitude and phase images can be drastically reduced, particularly in the center of the field of view. Intracranial aneurysms are mostly found at arterial branch points in the circle of Willis located in the subarachnoid space in the center of the brain [10]. PC-MRI image quality at this location may thus be compromised by a lower SNR due to parallel imaging acceleration.

An alternative acceleration technique is k-t BLAST [11]. This technique was developed for dynamic imaging, and acceleration is achieved by exploiting correlations in k-space and time. By means of simulations, the feasibility of k-t BLAST in combination with time-resolved three-dimensional PC-MRI has been shown by Marshall et al. [12]. Clinical studies using k-t BLAST in the carotid bifurcation [12], the aorta [13, 14], the myocardium [15] and the heart [16] showed that the technique leads to temporal blurring due to subtraction of a temporally averaged k-space from the data. However, other data showed minimal influence of temporal blurring [17, 18]. Furthermore, compared with SENSE, SNR may be higher in k-t BLAST accelerated PC-MRI as a consequence of limited temporal frequency content [19, 20].

This study presents a comparison between k-t BLAST and SENSE acceleration applied to time-resolved three-dimensional PC-MRI in an aneurysm as well as in a glass phantom of this aneurysm. Furthermore, we used the phantom for a comparison to non-accelerated 3D PC-MRI, a procedure that could not be applied to the patient due to long scanning time. Finally, we analyzed the effect of varying temporal resolution in the phantom. Our comparison includes the SNR and differences in velocity magnitude and direction between these acceleration techniques.

Materials and methods

In vivo aneurysm and phantom

A glass reproduction of an unruptured aneurysm located in the anterior communicating artery was manually blown by a glass-blower based on a 3D Rotational Angiography (3D-RA) dataset (Fig. 1a). Informed consent was given by this patient. The study protocol was approved by the local ethics committee. The lumen of the patient aneurysm had a maximum length, maximum width and maximum height of approximately 8, 6 and 9 mm in x, y and z directions, respectively (see Fig. 1a). The diameter of the neck of the aneurysm was approximately 2 mm. The lumen of the phantom had maximum dimensions of approximately 6, 4 and 9 mm in x, y and z directions, respectively (see Fig. 1b). The inner diameter of the in- and outflow vessels was 2.1 mm, and wall thickness was 0.2-0.6 mm in the inflow vessel, 0.4–0.6 mm in the outflow vessels and 0.8 mm in the phantom itself.

Phantom PC-MRI measurements

The flow loop consisted of the aneurysm phantom in a plastic box filled with agar gel, a reservoir, a centrifugal pump, a computer-controlled piston pump (pulse generator) and tubes, as displayed in Fig. 2. The dimensions of the agar block were: 7 cm in length, 5.5 cm in width and 3 cm in height. Pure water was used as a fluid. The combination of the centrifugal pump, delivering the steady mean flow, and the computer-controlled piston pump created the pulsatile flow used in the measurements. The MRI scanner used an artificial electrocardiogram signal to synchronize the PC-MRI acquisition with the flow pulses of the pump. The frequency of the pulses was set to 1 Hz to create a heart cycle duration of 1 s. Further information on this set-up can be found in [21].

Non-accelerated and SENSE accelerated scans were performed using a retrospectively gated [22] three-dimensional PC-MRI scan, whereas the k-t BLAST accelerated measurements were prospectively gated. A one-dimensional SENSE acceleration factor of 3 was applied in the right-left direction. An acceleration factor for the k-t BLAST acquisitions of 5 was set, to be able to acquire a temporal resolution of ten cardiac phases. This means that k-space was undersampled by taking every fifth k-line in the phase encoding direction. For each subsequent cardiac phase, the undersampling scheme was shifted up by one k-line. This acceleration factor did not take into account the acquisition of the training lines. Eleven training lines were acquired in the k-t BLAST measurements [23]. Therefore, the actual reduction in scan time was a factor of approximately 4 (see scan times in Table 1). Note that a SENSE
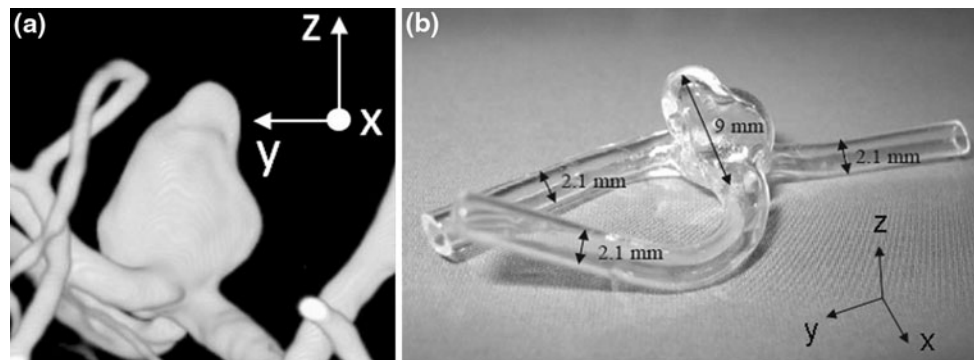
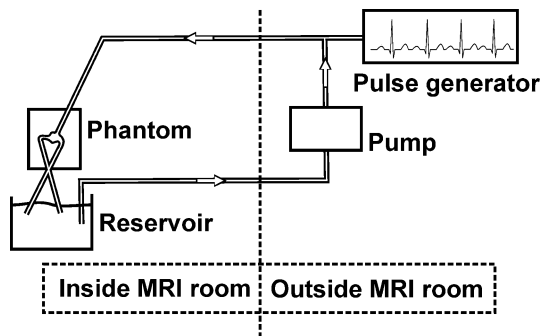Fig. 1 a The patient aneurysm as visualized by 3D-RA. b The aneurysm phantom

Fig. 2 The flow loop set-up

factor of 4 would result in equal scan time as the k-t BLAST measurements, but would further decrease SNR [24].

Three temporal resolutions were used: 10 cardiac phases or 100 ms, 20 cardiac phases or 50 ms and 40 cardiac phases or 25 ms. Sequence parameters for non-accelerated, k-t BLAST and SENSE accelerated measurements are summarized in Table 1. Further sequence parameters were: flip angle: 15°; field of view: $100 \times 100 \times 20$ mm^3; 25 coronal slices; velocity encoding (VENC): 80 cm/s $\times$ 120 cm/s $\times$ 80 cm/s in the x, y and z-direction, respectively (see Fig. 1b); NSA: 1. All PC-MRI scans were performed with one sided [25] four point encoding [7] on a 3T MR system (Philips Healthcare, Best, The Netherlands) in an 8-channel head coil at an acquired (non interpolated) resolution of $0.78 \times 0.78 \times 0.8$ mm^3.

In vivo aneurysm

Time-resolved 3D PC-MRI with SENSE and k-t BLAST acceleration was performed in the same patient of whom

the 3D-RA data was used to create the phantom. For both the SENSE and k-t BLAST acquisition, imaging parameters were: TE/TR: 2.8/5.6 ms, flip angle: 15°, acquired resolution: $0.78 \times 0.78 \times 0.8$ mm^3, 25 transversal slices, field of view: $200 \times 200 \times 20$ mm^3, velocity encoding: 100 cm/s $\times$ 100 cm/s $\times$ 100 cm/s in all three directions and NSA: 1. Ten cardiac phases were measured. The same 8-channel head coil as in the phantom scans was used. Scan time with a SENSE factor of 3 was 12 min. For the k-t BLAST acquisition with an acceleration factor of 5 and 11 training lines the scan time was 8 min, again an actual acceleration factor of 4. Non-accelerated measurements were not acquired.

Data analysis

Measured velocity encoded phase images were corrected for background phase by subtraction of the average phase in a region of interest in the agar gel close to the aneurysm phantom and the amygdala in the in vivo case. Phase correction was performed for every velocity encoding direction and cardiac phase individually [26]. The phantom lumen was segmented with the use of a level set evolution algorithm applied to the non-accelerated magnitude images at peak systole [27]. The in vivo aneurysm was segmented for every slice and cardiac phase individually. Pixels that suffered from velocity aliasing were manually corrected by adding two times VENC to aliased pixels with a velocity below zero and by subtracting two times VENC to aliased pixels with a velocity above zero. Signal to noise ratios were calculated in all PC-MRI acquisitions according to Price et al. [28], Dietrich et al. [29] and Plein et al. [30]. In short, let S_1 and S_2 represent magnitude signals in a ROI

Table 1 Measurement parameters for the full non-accelerated, k-t BLAST and SENSE measurements in the aneurysm phantom

	Non-accelerated	k-t BLAST	SENSE
TE/TR (ms)	3.2/5.9	2.9/6.1	3.2/5.9
Scan time 10/20/40 cardiac phases (min)	17/33/66	4/8/17	6/12/24

during different cardiac phases of similar mean velocity. These cardiac phases were chosen such that a subtraction of the images resulted in minimal signal. This was done for each dataset individually. SNR is then estimated from [31]:

$$\text{SNR} = \frac{\text{mean}(S_1 + S_2)|\text{ROI}}{\sqrt{2}\text{std}(S_1 - S_2)|\text{ROI}} \tag{1}$$

As ROI we chose the total aneurysm phantom and the aneurysm with connected arteries for the in vivo measurement. Since the SNRs of the magnitude and phase images are proportional [9, 32, 33] we did not separately estimate SNR in the phase images. Velocity to noise ratio (VNR) equals SNR times velocity divided by VENC. VNR was not calculated separately.

The mean velocity at peak systole and diastole were defined as the maximum and minimum of the mean velocity magnitude curve, respectively. The means of the paired differences between the full non-accelerated acquisition and the accelerated measurements were determined at peak systole and diastole by subtracting the velocity magnitude in corresponding voxels and subsequently averaging over the number of voxels. Standard deviations of the paired differences (SDp) at these cardiac phases were determined. Differences in flow direction were calculated from the angle difference between corresponding velocity vectors. Since these differences are positive by definition, median rather than mean values were calculated. Statistical comparison was done for paired groups (Wilcoxon-signed rank test) as data was not normally distributed. Differences were considered significant at $p < 0.05$. All post-processing steps and visualizations were performed with custom-built software in Matlab (Mathworks, Natick, MA, USA).

Results

Phantom measurements

Figure 3 shows three phase contrast magnitude images for the non-accelerated, *k-t* BLAST and SENSE measurement at 10 cardiac phases. The SNR of the non-accelerated measurements were 69, 75 and 72, the SNR of the *k-t* BLAST measurements were 94, 108 and 99 and the SNR of the SENSE measurements were 29, 31 and 30 for 10, 20 and 40 cardiac phases, respectively. The SNR degradation due to SENSE is clearly visible in Fig. 3c. Phase offsets close to the phantom (1 mm) before correction were low (<1.4 cm/s).

Figure 4 shows the mean velocity curves in the phantom for the non-accelerated, *k-t* BLAST and SENSE measurement. Mean peak systolic, diastolic velocity and the pulsatility are given in Table 2. Results of the statistical analysis are presented in Table 3. Application of the acceleration techniques resulted in altered estimates of mean velocity

magnitude as compared to the non-accelerated measurements (Fig. 4). Both acceleration techniques underestimated systolic velocity. This was particularly the case for *k-t* BLAST (Table 2). The differences between both acceleration techniques were also significant (Table 3). As a result of these deviations from non-accelerated measurements, systolic-diastolic pulsatility (last column in Table 2) is underestimated by notably the *k-t* BLAST technique, which can be attributed to temporal blurring. Temporal blurring was higher at 10 cardiac phases than 20 and 40. At 40 cardiac phases (Fig. 4c) the mean velocity curve derived from the SENSE measurement became less smooth than the non-accelerated and *k-t* BLAST mean velocity curve. This behavior was reported previously in the aorta at similar SENSE acceleration factors [9].

The above analysis quantifies systematic deviations in velocity resulting from the acceleration techniques. Table 3 indicates that the standard deviations of the paired differences and the median angle were similar for *k-t* BLAST and SENSE accelerated measurements. Note that the median angle increased in diastole compared to systole for all measurements. Since in diastole the velocities were generally lower than in systole the VNR decreased, introducing more uncertainty in direction of local flow.

Figure 5a, b and c show velocity field vectors in a sagittal plane through the phantom at peak systole for the non-accelerated measurement, *k-t* BLAST measurement and SENSE measurement, respectively, acquired at a temporal resolution of 100 ms. Figure 5 d, e and f show the velocity vectors at diastole. Qualitative similarities in velocity patterns such as the large vortex in the centre of the phantom and the small vortex at the upper left side of the phantom can be appreciated in Fig. 5. In Fig. 6 systolic transversal and coronal characteristic slices are displayed. The vortex on the right side (arrow 1) of the phantom in the transversal slices and the vortex in the tip of the aneurysm in the coronal slices (arrow 2) were well resolved for all three measurements. Quantitative differences can be appreciated for the *k-t* BLAST measurements, notably in the inflow region in systole (Figs. 5b, 6b, 6e). The lower velocity for *k-t* BLAST can be attributed to temporal blurring. In contrast, the velocity field vectors acquired with SENSE acceleration at systole (Figs. 5c, 6c, 6f) showed good similarity with the ones derived from the non-accelerated acquisition (Figs. 5a, 6a, 6d). In diastole the flow patterns were qualitatively and quantitatively similar for all methods.

In vivo aneurysm measurement

The SNR of the SENSE and *k-t* BLAST accelerated measurement was 12 and 21, respectively. Temporal blurring, i.e., underestimation of the mean velocity in systole,

Fig. 3 Phase contrast magnitude images for **a** the non-accelerated measurement, **b** the *k-t* BLAST measurement and **c** the SENSE measurement at 10 cardiac phases
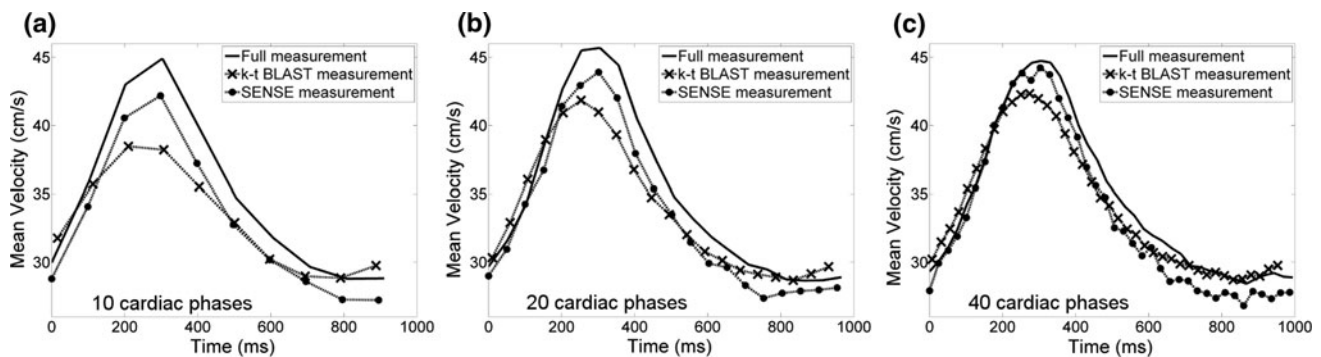

Fig. 4 Mean velocity curve in the phantom of the full non-accelerated, *k-t* BLAST and SENSE measurement at **a** 10 cardiac phases, **b** 20 cardiac phases and **c** 40 cardiac phases

Table 2 Mean velocity at systole and diastole and the difference

Nr of cardiac phases	Mean velocity systole (cm/s)			Mean velocity diastole (cm/s)			Difference/pulsatility (cm/s)		
	10	20	40	10	20	40	10	20	40
Non-accelerated measurement	45	46	45	29	29	28	16	17	17
k-t BLAST measurement	38	42	42	29	29	29	9	13	13
SENSE measurement	42	44	44	27	27	27	15	17	17

similar to the phantom measurement at 10 cardiac phases, occurred in the *k-t* BLAST measurement (Fig 7). Table 4 shows similar systematic and random differences between SENSE and *k-t* BLAST as was found for the phantom.

The directions of the velocity vectors in the SENSE and *k-t* BLAST accelerated measurement, displayed in Fig. 8a, b, respectively, showed many similarities. The large vortex in the centre of the aneurysm was found in both measurements. The magnitude of the velocity vectors in the *k-t* BLAST measurement was lower than in the SENSE measurement. This was seen earlier in the phantom measurements, and again resulted from temporal blurring. The SENSE measurement in diastole (Fig. 8c) suffers from low VNR, leading to irregularities in measured flow direction.

Due to higher SNR, this effect was less pronounced in the *k-t* BLAST measurement (Fig. 8d).

Discussion

In this study *k-t* BLAST and SENSE acceleration for time-resolved 3D PC-MRI in an intracranial aneurysm were compared, in vitro as well as in vivo. The main effect of *k-t* BLAST was temporal blurring. Acceleration using SENSE rendered more accurate velocity measurements in peak systole than *k-t* BLAST. Pulsatility of local flow and wall shear stress is considered to be an important causal factor in vascular pathology [34]. The diagnostic value of

Table 3 Difference between the non-accelerated and *k-t* BLAST measurement (first row), the non-accelerated and SENSE accelerated measurement (second row) and between the *k-t* BLAST and SENSE accelerated measurement (third row) in the phantom: mean of the paired difference where * indicates a significant difference, standard deviation of the paired difference (SDp) and the median of the angle at systole and diastole

Nr of cardiac phases	Mean paired difference systole (cm/s)			Mean paired difference diastole (cm/s)			SDp systole (cm/s)			SDp diastole (cm/s)			Median angle systole (°)			Median angle diastole (°)		
	10	20	40	10	20	40	10	20	40	10	20	40	10	20	40	10	20	40
k-t BLAST measurement	6.4* (p < 0.001)	3.8* (p < 0.001)	2.4* (p < 0.001)	−0.1 (p = 0.2)	−0.0 (p = 0.4)	−0.3* (p = 0.045)	10.4	10.2	14.8	5.8	6.3	9.4	8.9	10.3	11.3	9.7	11.0	12.9
SENSE measurement	2.7* (p < 0.001)	1.8* (p < 0.001)	0.5* (p < 0.001)	1.6* (p < 0.001)	1.3* (p < 0.001)	1.6* (p < 0.001)	10.1	11.5	18.3	5.9	6.0	9.8	8.7	7.9	12.2	10.8	10.9	13.1
k-t BLAST–SENSE	−3.7* (p < 0.001)	−2.1* (p < 0.001)	−1.9* (p < 0.001)	1.6* (p < 0.001)	1.3* (p < 0.001)	1.9* (p < 0.001)	11.9	13.2	12.8	6.9	7.8	7.6	10.1	12.3	11.5	12.1	15.4	12.7

3D PC-MRI could therefore suffer from the underestimation of peak velocities due to temporal blurring. The effect of temporal blurring could be diminished by increasing the number of cardiac phases, as was shown in the phantom measurements. For both the in vitro and in vivo case, good qualitative agreement between all measurements was found. As a result of temporal blurring and the high SNR of training data used for *k-t* BLAST reconstruction, a higher SNR was present in the *k-t* BLAST accelerated measurements as compared to SENSE.

The increased SNR for *k-t* BLAST may have been a consequence of the SNR calculation method used here. This method used two different cardiac phases to calculate the signal and the noise. Due to the temporal blurring effects in *k-t* BLAST, the noise calculation may present lower values and consequently higher SNR than in the non-accelerated and SENSE measurement. Furthermore, this method may not be appropriate when measuring at low temporal resolution, such as 10 cardiac phases. A possibly more accurate method to calculate SNR was presented by Kellman et al. [35]. This method requires additional measurements, which were not performed in this study. In the phantom study, the SNR of the SENSE measurement was approximately a factor 2.3 lower than that of the non-accelerated measurement. This number agrees well with the expected decrease in SNR with a factor of $g\sqrt{R} = 2.25$ [8], calculated using a *g*-factor of the 8-channel 3T coil array of 1.3 [36] and an acceleration factor $R = 3$. This data corroborates the SNR calculation method applied in this study.

The higher SNR found in this study for *k-t* BLAST may reflect a better reproducibility of *k-t* BLAST acceleration than SENSE acceleration. This can be beneficial in various situations where the precision of the measurement is more important than its accuracy, e.g., in longitudinal studies.

While the performance of *k-t* BLAST in intracranial aneurysms has not been studied in detail elsewhere, PC-MRI in combination with *k-t* BLAST in larger structures such as the carotid bifurcation [12], the aorta [13, 14] and the heart [16] suffered from temporal blurring as well as cardiac cine imaging [37] and quantification of myocardial motion [15]. Temporal blurring can be attributed to the view-sharing nature of *k-t* BLAST. However, the effect of temporal blurring was small in flow measurements accelerated with *k-t* BLAST in aortic valve stenosis [17]. Furthermore, by choosing sampling patterns with minimal signal overlap, temporal blurring can be slightly reduced [18]. Therefore, since the training data contains low resolution information of the imaging geometries, the temporal blurring effect may be more severe in the case of small structures such as aneurysms than in applications visualizing larger organs. The observed decrease in blurring at increased temporal resolution can be understood from

Fig. 5 Velocity magnitude and direction at systole (*top row*) and diastole (*bottom row*) in a sagittal slice through the phantom of **a**, **d** the non-accelerated acquisition **b**, **e** the *k-t* BLAST measurement and **c**, **f** the SENSE measurement. All pictures are obtained from the measurements in which 10 cardiac phases were acquired
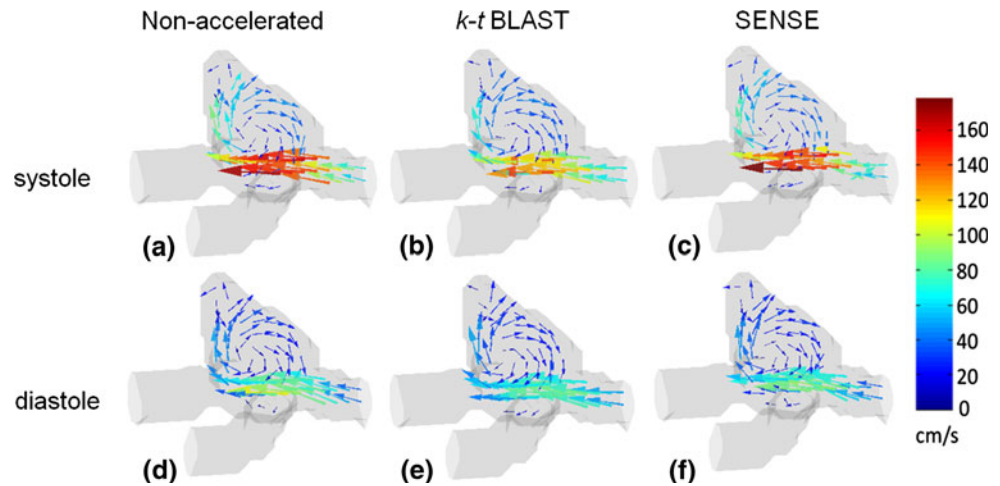

Fig. 6 Velocity magnitude and direction at systole in a transversal *top row* and coronal slice *bottom row* through the phantom of **a**, **d** the non-accelerated acquisition **b**, **e** the *k-t* BLAST measurement and **c**, **f** the SENSE measurement. All pictures are obtained from the measurements in which 10 cardiac phases were acquired
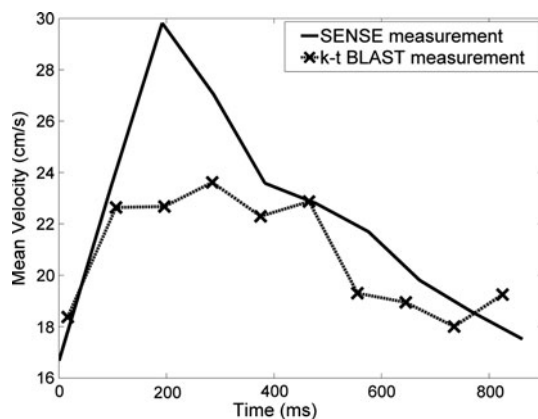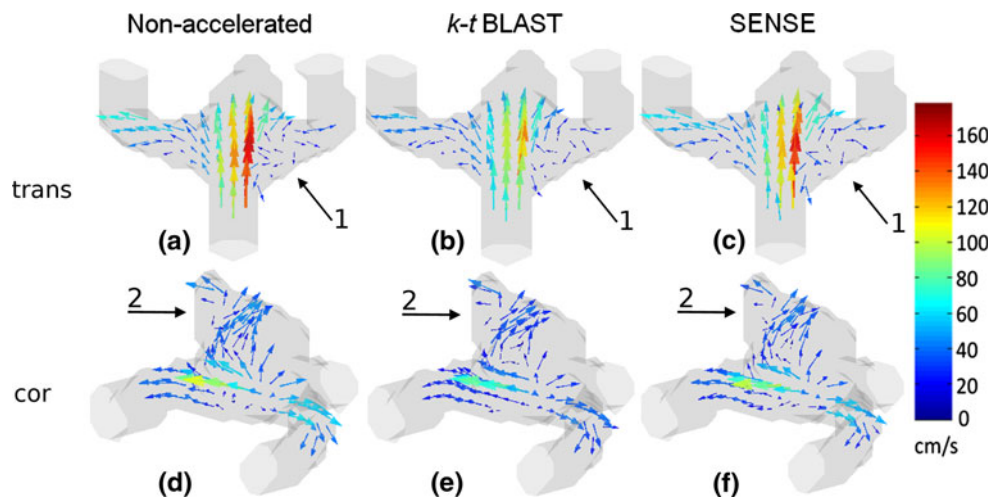

Fig. 7 Mean velocity curve in the patient aneurysm of the SENSE measurement and the *k-t* BLAST measurement

details of the *k-t* BLAST algorithm. An increase in temporal resolution will result in larger *x-f* arrays for the training and undersampled data, and will therefore contain more information on the unaliasing process, resulting in a more reliable *k-t* BLAST reconstruction [11].

Underestimation of velocities at peak systole may be unfavourable in aneurysmal rupture risk assessment since important risk factors as kinetic energy, strain rate and viscous dissipation of intra-aneurysmal blood flow depend on accurate velocity measurements or simulations [38, 39]. However, if one is only interested in a qualitative assessment of velocity patterns in intracranial aneurysms, *k-t* BLAST may be an attractive option since higher acceleration factors with preservation of SNR are possible compared to SENSE.

A limitation of the study was the fact that different acceleration factors were used for SENSE and *k-t* BLAST. The clinical protocol in our institution requires measurement of 10 cardiac phases. Therefore, a *k-t* BLAST acceleration factor of 5 was used since a factor 3 or 4 is not possible without altering the number of measured cardiac phases. This would imply that a SENSE factor of 4 should

Table 4 Mean velocity at peak systole and diastole, mean of the paired difference where * indicates a significant difference, standard deviation of the paired difference (SDp) and the median of the angle distribution between the SENSE measurement and the *k-t* BLAST measurement in the patient

	Mean paired difference systole (cm/s)	Mean paired difference diastole (cm/s)	SDp systole (cm/s)	SDp diastole (cm/s)	Median angle systole (°)	Median angle diastole (°)
k-t BLAST–SENSE	-5.7^* ($p < 0.001$)	1.7^* ($p < 0.001$)	8.9	7.2	19.5	28.6

Fig. 8 Velocity magnitude and direction at systole *top row* and diastole *bottom row* in a sagittal slice through the in vivo aneurysm of **a**, **c** the SENSE measurement and **b**, **d** the *k-t* BLAST measurement
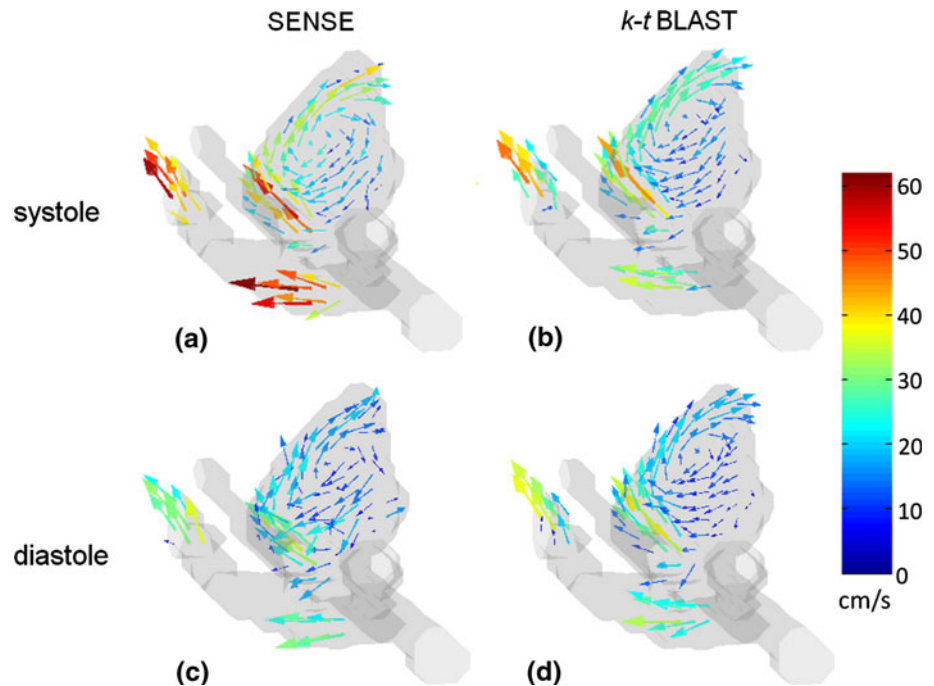
have been used to account for equal acceleration factors, which is not feasible when using an eight channel coil.

Further quantitative differences between *k-t* BLAST and SENSE in the in vivo setting can be attributed to the fact that the *k-t* BLAST measurement was prospectively gated, whereas the non-accelerated and SENSE measurements were retrospectively gated. The combination of retrospective gating and *k-t* BLAST acceleration was not available. By applying the shortest trigger delay timing in both the in vitro and in vivo measurements, differences between the two gating techniques in vitro, for the first and last (of ten measured) cardiac phases were limited. In the in vivo case the timing difference for the first and last cardiac phase was 16 and 37 ms, respectively. The time coverage of the total acquisition was therefore similar for both retrospective and prospective gating.

Only two acceleration techniques were studied. Other acceleration techniques exist, e.g., PC-VIPR [40], compressed sensing [41] and *k-t* PCA [42]. The latter technique showed less severe temporal blurring than *k-t* BLAST. These techniques are presently unavailable at our institution.

Conclusion

It was found that in systole, SENSE acceleration produces a more accurate result than *k-t* BLAST acceleration as a result of temporal blurring in an in vivo and in vitro aneurysm.

References

1. Proust F, Gerardin E, Chazal J (2008) Unruptured intracranial aneurysm and microsurgical exclusion: the need of a randomized study of surgery versus natural history. J Neuroradiol 35(2): 109–115
2. Spelle L, Pierot L (2008) Endovascular treatment of non-ruptured intracranial aneurysms: critical analysis of the literature. J Neuroradiol 35(2):116–120

3. Kayembe KN, Sasahara M, Hazama F (1984) Cerebral aneurysms and variations in the circle of Willis. Stroke 15(5):846–850

4. Chien A, Castro MA, Tateshima S, Sayre J, Cebral J, Vinuela F (2009) Quantitative hemodynamic analysis of brain aneurysms at different locations. AJNR Am J Neuroradiol 30(8):1507–1512

5. Wigstrom L, Sjoqvist L, Wranne B (1996) Temporally resolved 3D phase-contrast imaging. Magn Reson Med 36(5):800–803

6. Bammer R, Hope TA, Aksoy M, Alley MT (2007) Time-resolved 3D quantitative flow MRI of the major intracranial vessels: initial experience and comparative evaluation at 1.5T and 3.0T in combination with parallel imaging. Magn Reson Med 57(1):127–140

7. Pelc NJ, Bernstein MA, Shimakawa A, Glover GH (1991) Encoding strategies for three-direction phase-contrast MR imaging of flow. J Magn Reson Imaging 1(4):405–413

8. Pruessmann KP, Weiger M, Scheidegger MB, Boesiger P (1999) SENSE: sensitivity encoding for fast MRI. Magn Reson Med 42(5):952–962

9. Thunberg P, Karlsson M, Wigstrom L (2003) Accuracy and reproducibility in phase contrast imaging using SENSE. Magn Reson Med 50(5):1061–1068

10. Brisman JL, Song JK, Newell DW (2006) Cerebral aneurysms. N Engl J Med 355(9):928–939

11. Tsao J, Boesiger P, Pruessmann KP (2003) k-t BLAST and k-t SENSE: dynamic MRI with high frame rate exploiting spatio-temporal correlations. Magn Reson Med 50(5):1031–1042

12. Marshall I (2006) Feasibility of k-t BLAST technique for measuring "seven-dimensional" fluid flow. J Magn Reson Imaging 23(2):189–196

13. Stadlbauer A, van der Riet W, Crelier G, Salomonowitz E (2010) Accelerated time-resolved three-dimensional MR velocity mapping of blood flow patterns in the aorta using SENSE and k-t BLAST. Eur J Radiol 75(1):e15–e21

14. Stadlbauer A, van der Riet W, Globits S, Crelier G, Salomonowitz E (2009) Accelerated phase-contrast MR imaging: comparison of k-t BLAST with SENSE and Doppler ultrasound for velocity and flow measurements in the aorta. J Magn Reson Imaging 29(4):817–824

15. Lutz A, Bornstedt A, Manzke R, Etyngier P, Nienhaus GU, Rasche V (2011) Acceleration of tissue phase mapping by k-t BLAST: a detailed analysis of the influence of k-t-BLAST for the quantification of myocardial motion at 3T. J Cardiovasc Magn Reson 13:5

16. Carlsson M, Toger J, Kanski M, Bloch KM, Stahlberg F, Heiberg E, Arheden H (2011) Quantification and visualization of cardiovascular 4D velocity mapping accelerated with parallel imaging or k-t BLAST: head to head comparison and validation at 1.5 T and 3 T. J Cardiovasc Magn Reson 13:55

17. Thunberg P, Emilsson K, Rask P, Kähäri A (2012) Flow and peak velocity measurements in patients with aortic valve stenosis using phase contrast MR accelerated with k-t BLAST. Eur J Radiol 81(9):2203–2207. doi:10.1016/j.ejrad.2011.06.034

18. Tsao J, Kozerke S, Boesiger P, Pruessmann KP (2005) Optimizing spatiotemporal sampling for k-t BLAST and k-t SENSE: application to high-resolution real-time cardiac steady-state free precession. Magn Reson Med 53(6):1372–1382

19. Baltes C, Kozerke S, Hansen MS, Pruessmann KP, Tsao J, Boesiger P (2005) Accelerating cine phase-contrast flow measurements using k-t BLAST and k-t SENSE. Magn Reson Med 54(6):1430–1438

20. Tsao J, Tarnavaski O, Privetera M, Shetty S (2006) k-t denoising: exploiting spatiotemporal correlations for signal-to-noise improvement in dynamic imaging. Proceedings of the 14th annual meeting of ISMRM, Seattle, Washington, USA: 690

21. van Ooij P, Guédon A, Poelma C, Schneiders J, Rutten MCM, Marquering HA, Majoie CB, vanBavel E, Nederveen AJ (2012) Complex flow patterns in a real-size intracranial aneurysm phantom: phase contrast MRI compared with particle image velocimetry and computational fluid dynamics. NMR Biomed 25(1):14–26

22. Lenz GW, Haacke EM, White RD (1989) Retrospective cardiac gating: a review of technical aspects and future directions. Magn Reson Imaging 7(5):445–455

23. Hansen MS, Kozerke S, Pruessmann KP, Boesiger P, Pedersen EM, Tsao J (2004) On the influence of training data quality in k-t BLAST reconstruction. Magn Reson Med 52(5):1175–1183

24. de Zwart JA, Ledden PJ, Kellman P, van Gelderen P, Duyn JH (2002) Design of a SENSE-optimized high-sensitivity MRI receive coil for brain imaging. Magn Reson Med 47(6):1218–1227

25. Bernstein MA, Shimakawa A, Pelc NJ (1992) Minimizing TE in moment-nulled or flow-encoded two-and three-dimensional gradient-echo imaging. J Magn Reson Imaging 2(5):583–588

26. Lotz J, Meier C, Leppert A, Galanski M (2002) Cardiovascular flow measurement with phase-contrast MR imaging: basic facts and implementation. Radiographics 22(3):651–671

27. Li C, Xu C, Gui C, Fox MD (2005) Level set evolution without re-initialization: a new variational formulation. In: IEEE conference on computer vision and pattern recognotion (CVPR), San diego, USA, p 430–436

28. Price RR, Axel L, Morgan T, Newman R, Perman W, Schneiders N, Selikson M, Wood M, SR T (1990) Quality assurance methods and phantoms for magnetic resonance imaging: report of AAPM nuclear magnetic resonance Task Group No. 1. Med Phys 17(2):287–295

29. Dietrich O, Raya JG, Reeder SB, Reiser MF, Schoenberg SO (2007) Measurement of signal-to-noise ratios in MR images: influence of multichannel coils, parallel imaging, and reconstruction filters. J Magn Reson Imaging 26(2):375–385

30. Plein S, Ryf S, Schwitter J, Radjenovic A, Boesiger P, Kozerke S (2007) Dynamic contrast-enhanced myocardial perfusion MRI accelerated with k-t sense. Magn Reson Med 58(4):777–785

31. Reeder SB, Wintersperger BJ, Dietrich O, Lanz T, Greiser A, Reiser MF, Glazer GM, Schoenberg SO (2005) Practical approaches to the evaluation of signal-to-noise ratio performance with parallel imaging: application with cardiac imaging and a 32-channel cardiac coil. Magn Reson Med 54(3):748–754

32. Conturo TE, Smith GD (1990) Signal-to-noise in phase angle reconstruction: dynamic range extension using phase reference offsets. Magn Reson Med 15(3):420–437

33. Bernstein MA, Ikezaki Y (1991) Comparison of phase-difference and complex-difference processing in phase-contrast MR angiography. J Magn Reson Imaging 1(6):725–729

34. Satoh T, Omi M, Ohsako C, Katsumata A, Yoshimoto Y, Tsuchimoto S, Onoda K, Tokunaga K, Sugiu K, Date I (2005) Influence of perianeurysmal environment on the deformation and bleb formation of the unruptured cerebral aneurysm: assessment with fusion imaging of 3D MR cisternography and 3D MR angiography. AJNR Am J Neuroradiol 26(8):2010–2018

35. Kellman P, McVeigh ER (2005) Image reconstruction in SNR units: a general method for SNR measurement. Magn Reson Med 54(6):1439–1447

36. de Zwart JA, Ledden PJ, van Gelderen P, Bodurka J, Chu R, Duyn JH (2004) Signal-to-noise ratio and parallel imaging performance of a 16-channel receive-only brain coil array at 3.0 Tesla. Magn Reson Med 51(1):22–26

37. Kozerke S, Tsao J, Razavi R, Boesiger P (2004) Accelerating cardiac cine 3D imaging using k-t BLAST. Magn Reson Med 52(1):19–26

38. Cebral JR, Castro MA, Burgess JE, Pergolizzi RS, Sheridan MJ, Putman CM (2005) Characterization of cerebral aneurysms for assessing risk of rupture by using patient-specific computational

hemodynamics models. AJNR Am J Neuroradiol 26(10): 2550–2559

39. Mut F, Lohner R, Chien A, Tateshima S, Vinuela F, Putman C, Cebral J (2011) Computational hemodynamics framework for the analysis of cerebral aneurysms. Int J Numer Methods Biomed Eng 27(6):822–839

40. Chang W, Kecskemeti S, Frydrychowicz A, Landgraf B, Aagaard-Kienitz B, Wu Y, Johnson K, Wieben O, Mistretta C, Turski P (2011) Calculation of wall shear stress in intracranial cerebral aneurysms using high resolution phase contrast MRA

(PC-VIPR). Proceedings of the international society of magnetic resonance in medicine 19:3307

41. Hsiao A, Lustig M, Alley MT, Murphy M, Vasanawala SS (2011) Quantitative assessment of blood flow with 4D phase-contrast MRI and autocalibrating parallel imaging compressed sensing. Proceedings of the international society of magnetic resonance in medicine 19:1190

42. Pedersen H, Kozerke S, Ringgaard S, Nehrke K, Kim WY (2009) k-t PCA: temporally constrained k-t BLAST reconstruction using principal component analysis. Magn Reson Med 62(3):706–716